Hindawi Publishing Corporation
International Journal of Photoenergy
Volume 2014, Article ID 839757, 13 pages
http://dx.doi.org/10.1155/2014/839757

Research Article

Development of Dye-Sensitized Solar Cells with Sputtered N-Doped TiO_2 Thin Films: From Modeling the Growth Mechanism of the Films to Fabrication of the Solar Cells

D. A. Duarte,[1] M. Massi,[1,2] and A. S. da Silva Sobrinho[1]

[1] *Plasmas and Processes Laboratory, Technological Institute of Aeronautics, São José dos Campos 12228-900, SP, Brazil*
[2] *Institute of Science and Technology, Federal University of São Paulo, São José dos Campos 12245-000, SP, Brazil*

Correspondence should be addressed to D. A. Duarte; diegoalexandreduarte@gmail.com

Received 7 May 2013; Accepted 7 January 2014; Published 25 February 2014

Academic Editor: Cooper H. Langford

In this paper, nitrogen-doped TiO_2 thin films were deposited by DC reactive sputtering at different doping levels for the development of dye-sensitized solar cells. The mechanism of film growth during the sputtering process and the effect of the nitrogen doping on the structural, optical, morphological, chemical, and electronic properties of the TiO_2 were investigated by numerical modeling and experimental methods. The influence of the nitrogen doping on the working principle of the prototypes was investigated by current-voltage relations measured under illuminated and dark conditions. The results indicate that, during the film deposition, the control of the oxidation processes of the nitride layers plays a fundamental role for an effective incorporation of substitutional nitrogen in the film structure and cells built with nitrogen-doped TiO_2 have higher short-circuit photocurrent in relation to that obtained with conventional DSSCs. On the other hand, DSSCs built with nondoped TiO_2 have higher open-circuit voltage. These experimental observations indicate that the incorporation of nitrogen in the TiO_2 lattice increases simultaneously the processes of generation and destruction of electric current.

1. Introduction

Since the dye-sensitized solar cells (DSSCs) were introduced by O'Regan and Graetzel in the early 90s [1] several studies were conducted aiming to improve the light-to-electricity conversion of the DSSCs by modifying various cell components, including the transparent conductive oxides [2], light absorbers [3], redox electrolytes [4], counter-electrodes [5], and the TiO_2 structure [6–8]. In 2001, Asahi and coauthors [9] reported a theoretical study in which they simulated the doping of the TiO_2 with several metal and nonmetal anions in order to red-shift its optical absorption once this material can absorb only UV light due to its wide band gap. In their studies, it was verified that the substitutional doping with nitrogen was more effective to decrease the energy band gap of the TiO_2 due to the insertion of N2p states above the top of valence band. Since then, many experimental investigations have been published on this issue, so that, a large number of works have applied this improved material to study the DSSC technology. Kang and coauthors [10], for example, reported that the nitrogen-doped titania electrode-based DSSCs showed superior efficiency relative to that attained with pure titania. Ma and coauthors [11] found similar results. Lindgren and coauthors [12] reported that nitrogen-doped TiO_2 electrode-based DSSC displayed an improved incident photon to electron conversion efficiency (IPCE) relative to that obtained with undoped TiO_2 electrode.

Nitrogen-doped TiO_2 can be deposited as crystalline or amorphous structure where the overall composition is often a mixture between TiN, TiO_2 and suboxides like TiO, Ti_2O_3, and Ti_3O_5. However, Hashimoto and coauthors [13] found that TiO and Ti_2O_3 are the most predominant suboxides obtained during the reactive sputter deposition of TiO_2. In addition, XPS analyses [14, 15] revealed substitutional and

interstitial nitrogen incorporated in the TiO_2 lattice, which is in agreement with the theoretical investigations conducted by Asahi et al. [9].

According to Jiang and coauthors [16] nitrogen-doped TiO_2 can be prepared from incorporation of nitrogen atoms in the TiO_2 lattice or oxidation of TiN. In the first case, nitrogen is usually incorporated by sol-gel method [17], chemical-vapor deposition [18, 19],and hydrothermal and solvothermal synthesis [20–22]. The other one can be ascribed, for example, by oxidation of TiN at high temperatures [23] and micro-arc oxidation from ion beam-assisted deposition [24]. However, nitrogen incorporated in the stoichiometric TiO_2 from chemical methods, for example, requires high energy because the Ti–O bonds are difficult to be broken by nitrogen atoms [16]. As a result, the overall film structure, in this case, becomes interstitially doped and the energy band gap, as well as, the optical absorption remains approximately unaltered. The second case, oxidation of TiN, is a more efficient method for incorporation of substitutional nitrogen due to the facility of the Ti–N bonds to be broken by oxygen [16]. However, some experimental investigations [25, 26] reported a sudden reduction in the energy band gap of nitrogen-doped TiO_2 prepared by reactive sputtering once this technique combines the oxidation of TiN and chemisorption of reactive gas particles [27].

Nitrogen-doped TiO_2 prepared by reactive sputtering is generally deposited from a metallic titanium target immersed in a reactive gas mixture of argon, nitrogen, and oxygen [12, 25, 26, 28, 29]. In some cases, the exchange of oxygen by water vapor has been also used as an alternative [30]. In the most cases, nitrogen-doped TiO_2 is usually deposited by assuming high nitrogen concentration mixed with low oxygen concentration. This procedure induces first the growth of nitride layers to later be oxidized by oxygen particles, thereby improving the incorporation of the nitrogen particles in the film lattice. Large amounts of oxygen mixed with small amounts of nitrogen lead to a poor incorporation of nitrogen particles in the film lattice or not as efficient as it should be. See studies conducted in [25, 28].

A correct understanding of the effects that lead to an effective incorporation of nitrogen particles in the TiO_2 lattice is not always an easy task from experimental methods. Sometimes the correlation of the experimental results with numerical data, for example, can help us to clarify some details not achievable in laboratory. For this, it is necessary to use a reliable model that describes consistently all necessary parameters during film deposition. In this way, the so-called Berg model [31] shows to be interesting on this issue due to its capacity to describe adequately all experimental parameters during the deposition process. Previous studies based on Berg's model and conducted by our group [32] show that there is an optimal gas mixture for deposition of nitrogen-doped TiO_2 by reactive sputtering in which the band gap is reduced. This finding is consistent with several experimental results obtained elsewhere. However, more studies are needed about this subject, mainly studies related to the effects that lead to the incorporation of substitutional nitrogen during the temporal evolution of the growing film.

In this paper, nitrogen-doped TiO_2 thin films were deposited by DC reactive sputtering and used for fabrication of dye-sensitized solar cells. The general effects of nitrogen incorporation on the film properties, as well as, its influence on the working mechanism and performance of the solar cells were promptly investigated. In addition, an original numerical model was used to simulate the reactive sputter deposition of nitrogen-doped TiO_2 in order to study the growth mechanism of the films and understand how the substitutional nitrogen is incorporated in the film lattice during the reactive deposition.

2. Experimental Setup and Model Input Data

Nitrogen-doped TiO_2 thin films were deposited by DC reactive magnetron sputtering using a planar magnetron with a titanium disk (99.6%) of 34 mm in diameter as target. Films were deposited at different oxygen flow rates (0.2, 0.6, 0.9, 1.3, 1.7, 2.2, 2.6, 3.0, and 3.5 sccm) on grounded glass substrates coated with fluorine-tin oxide (FTO). Other experimental parameters such as argon flow rate, nitrogen flow rate, DC power, and target-to-substrate distance were fixed at 10 sccm, 10 sccm, 150 W, and 30 mm, respectively. After deposition process, they were analyzed by profilometry, X-ray diffraction (XRD), optical spectrophotometry, atomic force microscopy (AFM), Rutherford backscattering spectroscopy (RBS), and X-ray photoelectron spectroscopy (XPS). The energy band gap of the films was calculated from Tauc relation for indirect semiconductors [28] and the absorption coefficient, used in the Tauc's plot, was taken from relation used in [12]. Profilometry data were used to calculate the energy band gap and will not be shown. Film thicknesses were fixed at 2 μm. It must be cleared that the XPS technique was used to investigate the chemical composition of the films surface and the RBS technique was used to investigate the bulk.

The numerical model used in this paper and all necessary parameters used during the simulations are described in details according to [32]. In summary, the model is represented by a set of ordinary differential equations that describe the reactions of destruction and formation of compound on the target and substrate. Solving these sets of nonlinear equations gives the chemical composition on the target and substrate in either stationary or nonstationary conditions. In the present study, we will conduct simulations only in the nonstationary region. Studies about the stationary condition were conducted in the above-referenced study.

DSSCs were built in a conventional sandwich-type-two-electrode cell as detailed in [1]. The working electrodes were built from deposition of nitrogen-doped TiO_2 on FTO substrates according to described previously. The counter electrodes were built from FTO substrates coated with graphitized carbon films according to experimental details given in [33]. Sensitization of TiO_2 and nitrogen-doped TiO_2 was made with 0.25 mMol/L of cisdithiocyanato-bis(2,2′-bipyridyl-4,4′-dicarboxylate)-ruthenium (II) diluted in 60 mL of ethanol. Prior to the sensitization, films were annealed for 400°C in high vacuum (~10^{-5} Torr) for 1 hour and dipped into the dye solution while they were still warm (80°C) and kept immersed by 24 hours. After the soaking

process, the electrodes were light purple. Sealing was done with 25 μm thick thermoplastic hot-melt sealing foil and all electrical contacts were improved with silver paint. The effective area of the cells was fixed at 2.25 cm^2 (0.5 × 4.5 cm^2). After finishing all these steps , they were characterized under irradiation of an Oriel Xe (Hg) 250 W lamp with AM 1.5 filter, used to simulate the solar spectrum at 1 sun. The light intensity was adjusted using a Newport Optical Power Meter. Current-voltage relations were obtained using linear sweep voltammetry at 1 mV s^{-1} using an Eco Chemie-Autolab PGSTAT 10 potentiostat.

3. Results and Discussions

The results from XPS are summarized in Figures 1 and 2. Figure 1 shows the Ti2p core level for films deposited at O_2 flow rate of 0.2, 0.6, and 3.5 sccm. All spectra were decomposed in three characteristic contributions: $Ti^{2+}2p_{3/2}$, $Ti^{3+}2p_{3/2,}$ and $Ti^{4+}2p_{3/2}$. These peaks are, respectively, assigned to TiO, $Ti_2O_{3,}$ and TiO_2 [34, 35]. However, for titanium oxynitride-like structures, TiO cannot be clearly distinguished by XPS because the peak $Ti^{2+}2p_{3/2}$ is also assigned to TiN [25]. The increase of the peak $Ti^{4+}2p_{3/2}$ and decrease of the other ones, with increased O_2 flow rate, indicate the full oxidation of the film surface and, as consequence, formation of TiO_2.

The N1s core level is depicted in Figure 2. The results indicate a characteristic peak at about 396 eV for all spectra. According to fundamental studies, this peak is assigned to the substitutional nitrogen and it is generally known as "nitride" peak due to the substitution of O^{2-} by N^{2-} in the TiO_2 lattice giving the so-called O–Ti–N structure [14]. Other peaks between 398 and 402 eV were also detected by XPS and according to Saha and Tompkins they are related to chemisorbed N_2 at the grain boundaries [14]. However, Sato and coauthors [17] claim that the assignments of N1s peaks at 400 and 402 eV, for example, are implausible at room temperature because molecular N_2 cannot be chemisorbed on metal oxides like TiO_2. Since then , several studies stated that these peaks are assigned to different other forms of interstitial nitrogen as, for example, nitric oxides (NO_x) or other related chemical states like NC and NH_3 [36–39]. Thus, we consider that the peaks between 398 and 402 eV are related to interstitial nitrogen.

The XPS profiles show two peaks assigned to Ti–N bound in Figure 2(a). The first, detected at 395.7 eV, is ascribed to the Ti–N bound in nitride layers and the second one, detected at 396.8 eV, is assigned to the substitutional nitrogen in the TiO_2 lattice. However, as the O_2 flow rate increases, the binding energy associated to the Ti–N bound at 395.7 eV is shifted to 396 and, then, to 396.3 eV. See Figures 2(b) and 2(c), respectively. According to Chen and Burda [40], the electron density around to the nitrogen atoms is reduced upon oxidation of the nitride layers. This is caused by the high oxygen electronegativity: therefore, the N1s binding energy in the O–Ti–N structure becomes higher than in the N–Ti–N structure. By this way, this result shows that the oxidation of TiN changes the chemical state of the nitrogen from a simple chemisorbed particle in nitride layers to a dopant in the TiO_2 structure.

The results from numerical modeling for films deposited at O_2 flow rates of 0.2 and 3.5 sccm are shown in Figures 3(a) and 3(b), respectively. These graphs show the normalized deposition rate. For film deposited at O_2 flow rate of 0.2 sccm (Figure 3(a)) one can observe four well-defined stages. (i) Initially, after the discharge breakdown, particles of the reactive gases (N and O) react by chemisorption with Ti particles already deposited at the substrate for compound formation. (ii) After occupation of all available sites in the film structure, the chemisorption rate of the nitrogen and oxygen particles is reduced. At this stage, the target becomes poisoned due to the compound formation on it. As consequence, the sputtering yield as well as the flux of Ti particles toward the substrate decreases [32]. At stage (iii), the oxygen concentration increases again due to the oxidation of the nitride layers through the reaction $TiN + O_2 \rightarrow TiO_2 + (1/2)N_2$ where the amount of nitrogen released back again to the gas phase and the remaining one becomes trapped as substitutional or interstitial doping. At stage (iv), the system becomes stationary. The same mechanism occurs during deposition at O_2 flow rate of 3.5 sccm. However, due to the high O_2 concentration, the effect related to the oxidation process becomes more intense, thus eliminating almost by complete the amount of nitrogen in the film structure; see Figure 3(b).

The explanations for stages (i), (ii), and (iii), in Figure 3(b), are the same used for Figure 3(a). At stage (iv), a larger amount of nitrogen is released from film structure due to the higher O_2 concentration in the gas phase. In addition, the lowering in the chemisorption rate of the oxygen particles on the substrate is caused by decreasing of the Ti flux from the target. At stage (v), the system becomes stationary.

According to all these observations, the oxidation of the nitride layers seems to be the main responsible by eliminating the nitrogen particles of the film structure so the correct control of this parameter may result in better doping levels [32]. To exemplify the influence of the oxidation of the nitride layers on the chemical composition of the films, see Figure 4. In this figure, only the normalized deposition rate for nitrogen and oxygen is shown and calculations were done at O_2 flow rate of 3.5 sccm for cases with and without oxidation of TiN. Notice that the modeling without oxidation of the nitride layers is unreal. We are just using it to exemplify the importance of the oxidation process during film growing. The results show that profiles, with and without oxidation, are quite different. In the case for oxidation of TiN (Figure 4(a)), the remaining amount of nitrogen, in the stationary region, is lower than that obtained in the case without oxidation of TiN (Figure 4(b)) and the amount of oxygen in the case with oxidation of TiN is higher than that obtained in the case without the oxidation process. The results from numerical data employing oxidation of TiN are in agreement with XPS findings.

Based on these achievements, a standard growth mechanism can be described; see Figure 5. After deposition of the nitride layers, O atoms diffuse in the TiN lattice and replace N by O [41], thereby increasing the fraction of suboxides

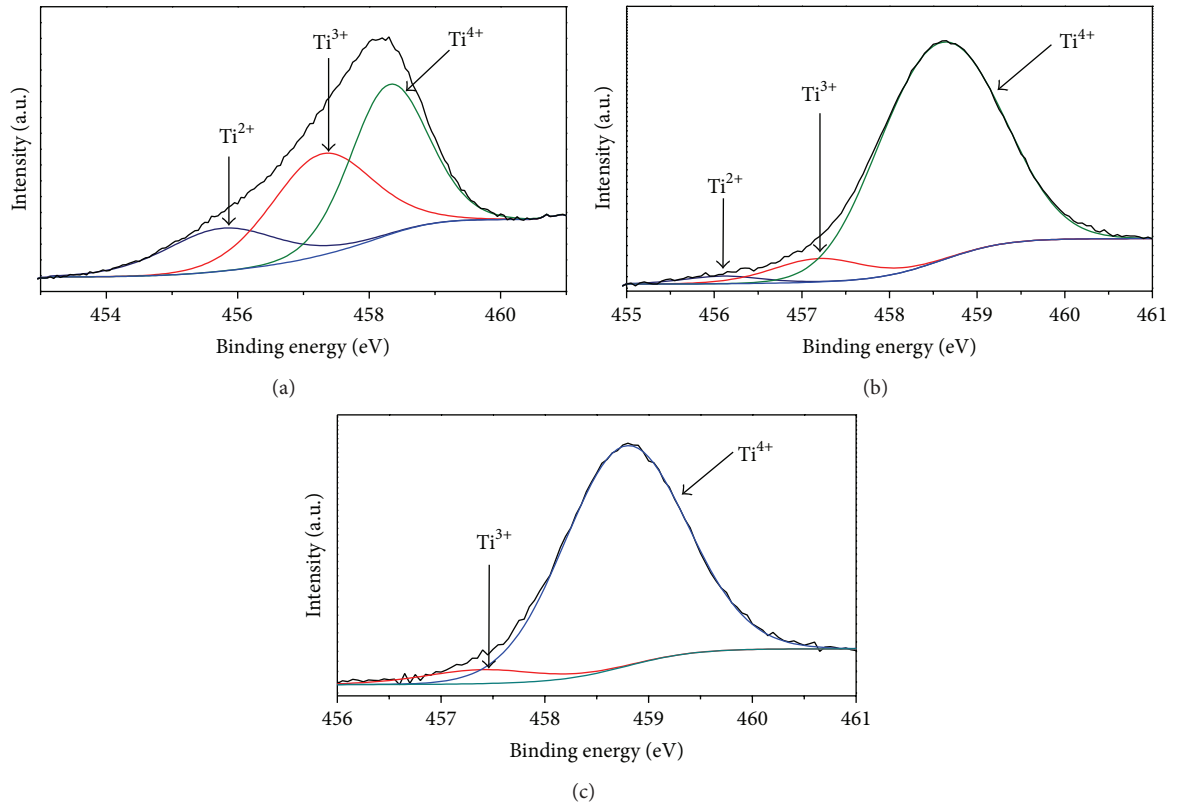

Figure 1: XPS spectra for Ti2p$_{3/2}$ core level of the films deposited at (a) 0.2, (b) 0.6, and (c) 3.5 sccm.

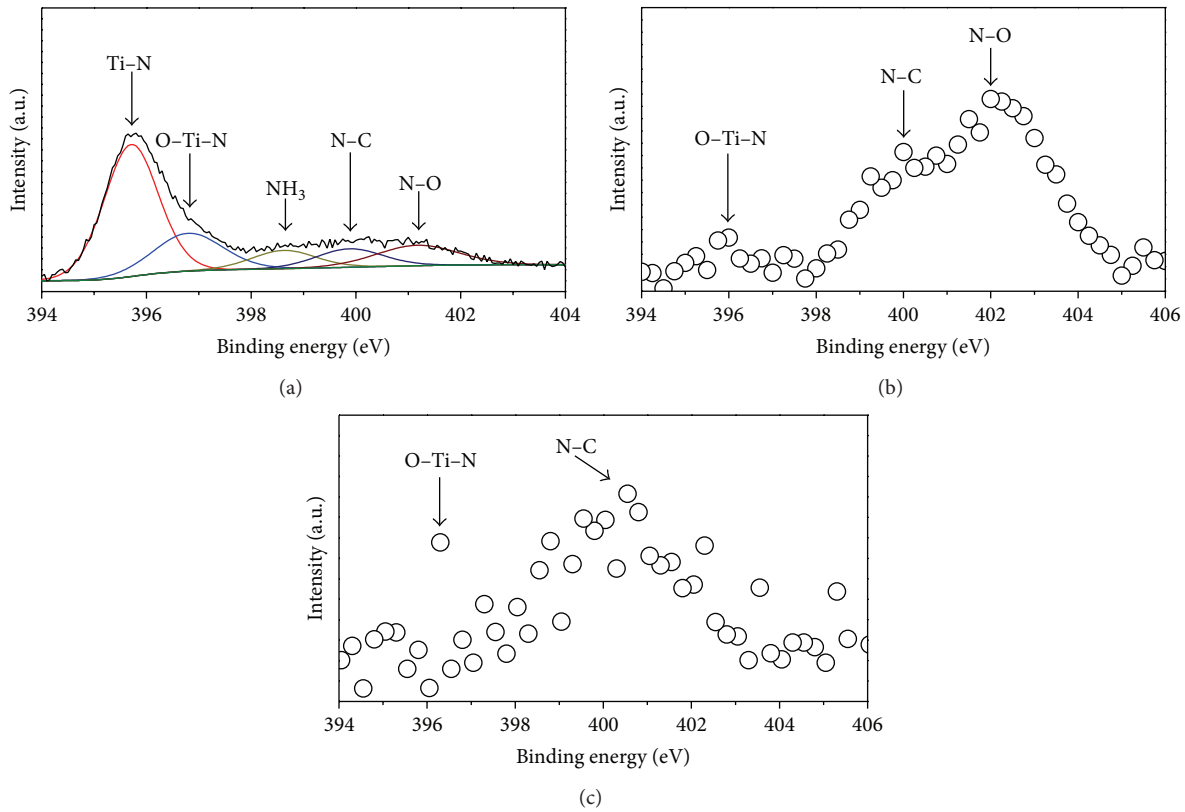

Figure 2: XPS spectra for N1s core level of the films deposited at (a) 0.2, (b) 0.6, and (c) 3.5 sccm.

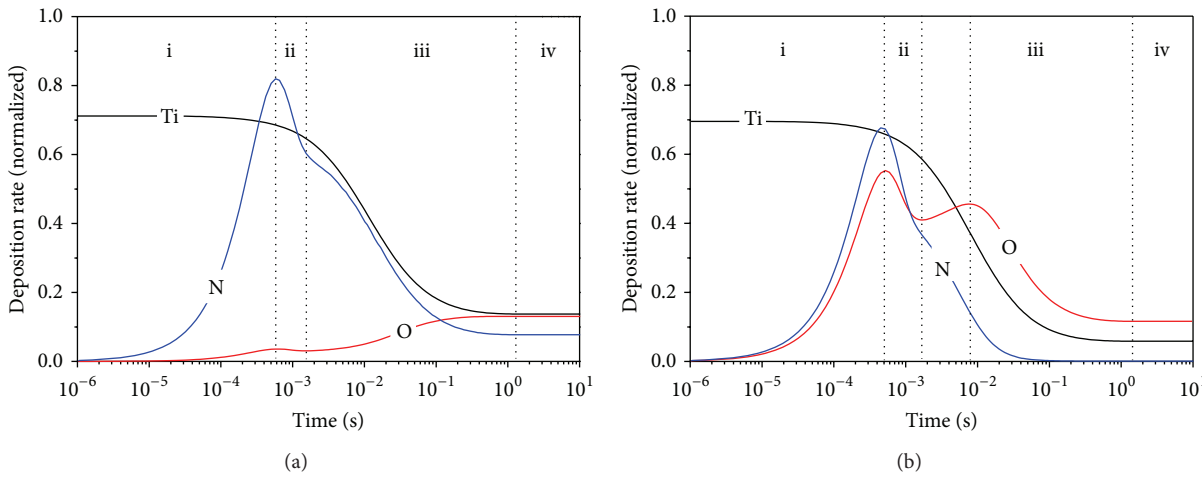

FIGURE 3: Deposition rate at oxygen flow rate of (a) 0.2 and (b) 3.5 sccm.

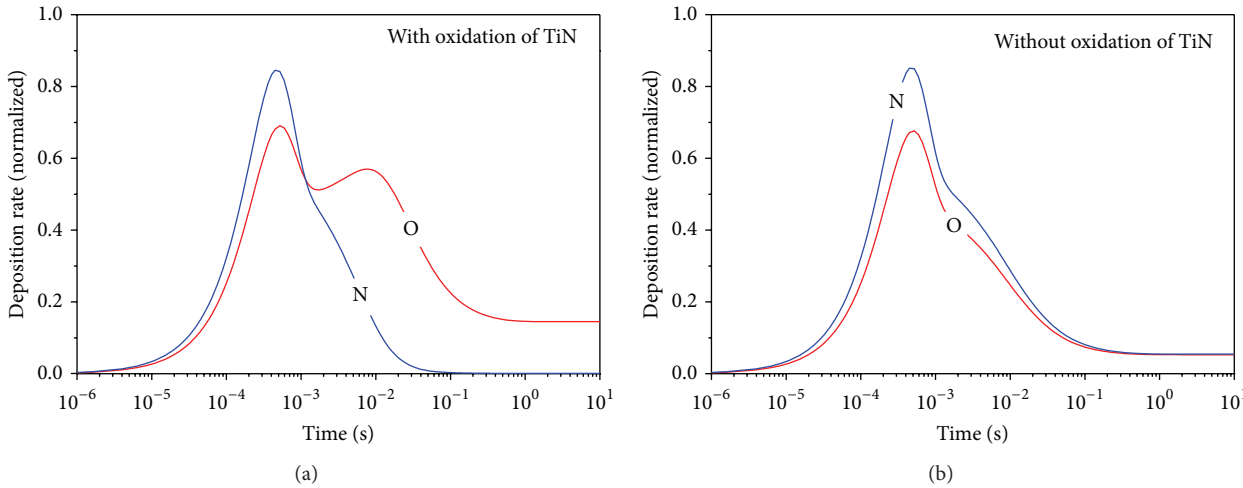

FIGURE 4: Deposition rate at oxygen flow rate of 3.5 sccm for the cases (a) with and (b) without oxidation of the nitride layers.

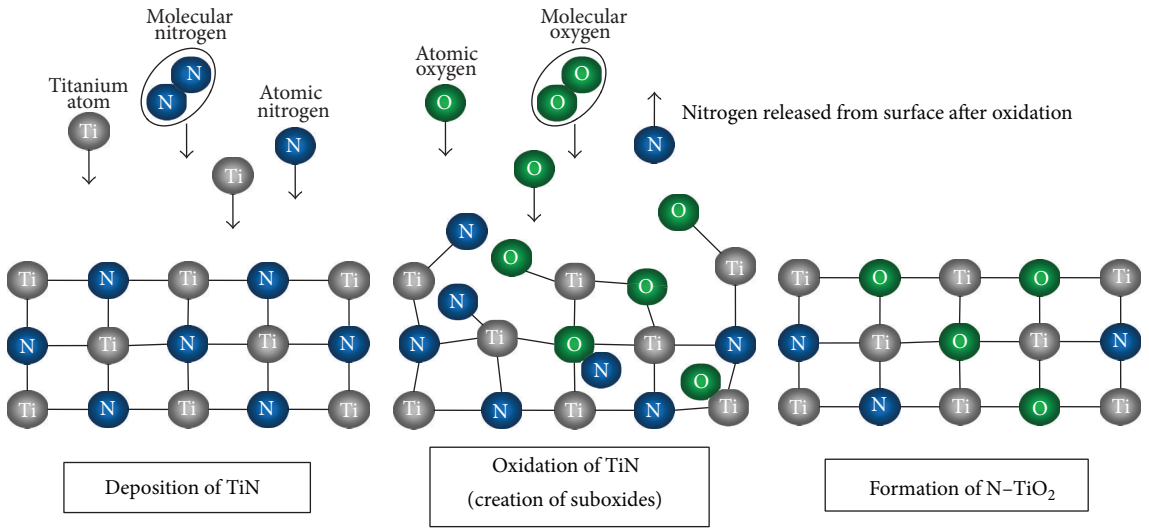

FIGURE 5: Growth mechanism for nitrogen-doped TiO_2 thin films deposited by DC reactive sputtering.

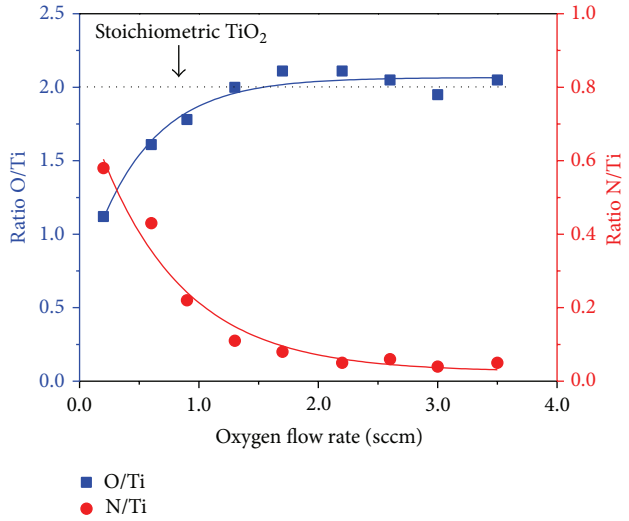

FIGURE 6: Chemical composition of the films obtained by RBS as function of the oxygen flow rate (reproduced from [32]).

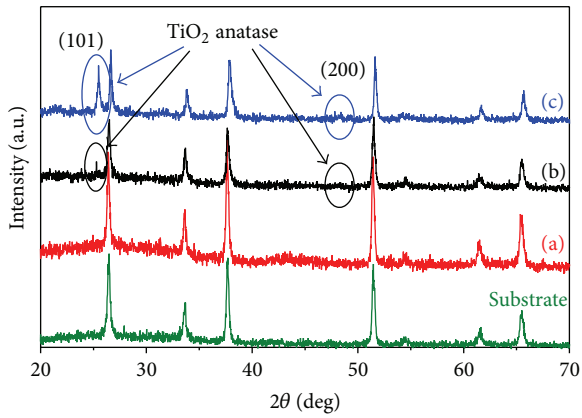

FIGURE 7: XRD patterns for films deposited at (a) 0.2, (b) 0.6, and (c) 3.5 sccm.

[42] and enabling nitrogen particles to be incorporated as substitutional doping in the voids of the film lattice [43]. In addition, the reaction between O and sputtered Ti followed by reaction with N is another path for incorporation of substitutional nitrogen, but, at low O_2 flow rates, this reaction is expected to be negligible [32]. On the other hand, as the O_2 flow rate increases, oxygen tends to react with suboxides more easily than nitrogen due to its higher sticking coefficient, and as consequence, the substitutional N concentration decreases and film becomes mostly covered by TiO_2 [32].

The chemical composition of the films obtained by RBS is shown in Figure 6. Similar results for oxynitride-like layers were observed elsewhere [26–28, 43]. At high O_2 flow rates, a decrease in the nitrogen concentration and the increase of oxygen content in the film composition were observed. According to studies conducted in the past, this increased oxygen content is assigned to oxidation of TiN [26, 44], thereby being in agreement with the results of the numerical model. In addition, the results indicate a ratio O/Ti < 2 for films deposited at 0.2, 0.6 and 0.9 sccm. This result suggests the existence of suboxides and, as consequence, O vacancies in the film bulk, although this result may be also ascribed to substitution of O by N in the TiO_2 structure. The presence of O defects in the bulk and surface of the films was investigated as described to follow.

The origin of Ti^{3+} is related to the existence of O vacancies in the bulk and surface, so each vacancy reduces two adjacent Ti atoms from Ti^{4+} to Ti^{3+}. Thus, the small intensity of active states Ti^{3+} in Figure 1(c) is likely attributed to the existence of O vacancies on film surface once RBS data, for the same film, show a ratio O/Ti = 2.05 so that it indicates that the bulk is stoichiometric. On the other hand, the presence of active states Ti^{3+} in Figures 1(a) and 1(b) may be ascribed, for example, to the existence of O vacancies in either bulk or surface once the ratio O/Ti is lower than 2 for these two films. According to XRD spectra depicted in Figure 7, film deposited at 0.2 sccm is amorphous. This means that the bulk and surface of this film have O deficiency. On the other hand, films deposited at 0.6 and 3.5 sccm are crystalline, which indicates a bulk without excessive vacancies. Thus, the ratio O/Ti < 2 for film deposited at 0.6 sccm is an indicative that the voids in the TiO_2 lattice were efficiently occupied by substitutional nitrogen so that the presence of O vacancies in this structure is mainly attributed to surface defects. These appointments are summarized in Table 1.

The effect of nitrogen doping on the energy band gap and refractive index is shown in Figure 8(a). The refractive index was calculated from the Moss rule [45]. The results indicate a decrease in the energy band gap as the O_2 flow rate decreases. Similar behavior was observed in other publications [25, 26]. The lowest energy band gaps of 1.9 and 2.5 eV were attained for films deposited at 0.2 and 0.6 sccm, respectively. As mentioned previously, this is caused by insertion of midgap states above the valence band of the films [9]. The highest energy band gaps of 3.2 eV were measured for films deposited at high O_2 flow rates. These values correspond to the energy band gap of pure anatase TiO_2, which is in agreement with XRD analysis. This result indicates that these films were not effectively doped with nitrogen, although XPS has detected a tiny concentration of substitutional nitrogen (see Figure 2(c)). The refractive index of the nitrogen-doped TiO_2 films has achieved values above 2.6 and, as the film surface is oxidized, it decreases toward the typical values of undoped anatase TiO_2. Similar behavior was also observed elsewhere [25, 26].

As shown in Figure 8(b), the energy band gap decreasing is not only caused by incorporation of N2p states. The absorption coefficient for film deposited at 0.2 sccm, for example, increases for wavelength above 525 nm. According to Fujishima and coauthors [46], this effect is a typical feature caused by excessive presence of Ti^{3+} states below the conduction band. The energy states caused by these active sites are reported to lie about 0.75 and 1.18 below the conduction band [47]. This observation, raised by Fujishima and coauthors, is in agreement with XPS and RBS analyses . The other films deposited at 0.6 and 3.5 sccm have, respectively, the characteristic absorption coefficients of nitrogen-doped and

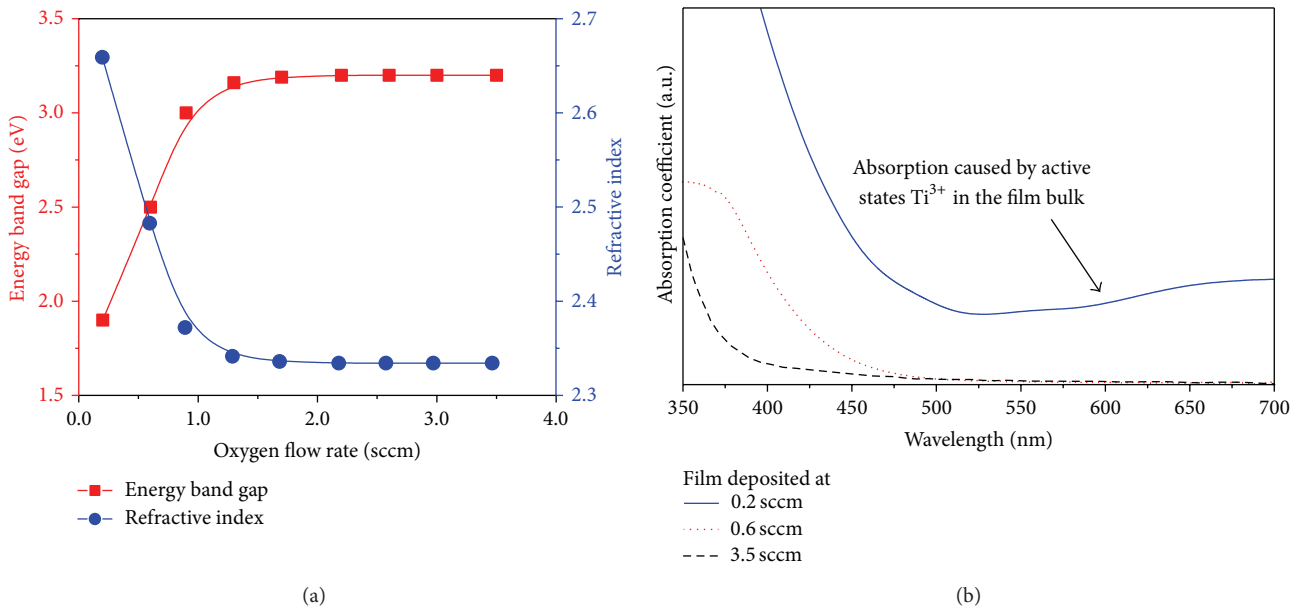

FIGURE 8: Energy band-gap (reproduced from [32]) and refractive index as function of the oxygen flow rate and (b) absorption coefficient for films deposited at 0.2, 0.6, and 3.5 sccm as function of photon wavelength.

TABLE 1: Structural properties of the films.

Deposition condition (Oxygen flow rate)	Structure	Crystal type	Oxygen defects	
			Bulk	Surface
0.2 sccm	Amorphous	—	Yes	Yes
0.6 sccm	Crystalline	Anatase	No	Yes
3.5 sccm	Crystalline	Anatase	No	Yes

undoped TiO_2 [46, 48]. Since there is no increase in the absorption coefficient for films deposited at 0.6 and 3.5 sccm, we can conclude that the increase of the absorption coefficient in the near-infrared part to the film deposited at 0.2 sccm is caused by the active states Ti^{3+} in the film bulk.

All films were deposited with (101) and (200) preferred orientation. XRD spectra before and after annealing do not show any difference between each other, which indicates crystallization during film deposition. The preferential anatase crystallization for TiO_2 thin films deposited by conventional magnetron sputtering has been discussed in a previous study [49]. The other diffraction peaks are associated with the substrate. In overall, a decrease in the diffraction peak of the anatase phase is observed as more nitrogen is incorporated in the film lattice. This effect has been also reported by our group in a previous publication [50]. Other studies observed similar results [28, 51]. According to Muscat and coauthors [52], the excessive nitrogen incorporation elevates the density of the TiO_2 matrix by their volume, which may act as a driving force of the structural phase transformations. Other papers [26, 53, 54] reported that nitrogen acts as a crystallization inhibitor once nitrogen incorporated in the TiO_2 lattice decreases the mobility of Ti and O atoms, and,as a consequence, the nucleation of crystalline phases is reduced. They claim that this effect is caused by the larger ionic radius of N as compared with O.

The effect of nitrogen doping on the working principle of solar cells was evaluated from current-voltage relations measured under illuminated and dark conditions. For convenience, cells built with films deposited at 0.2, 0.6 and 3.5 sccm will be called cells A, B, and C, respectively. Cells parameters like the short-circuit current density (J_{SC}), open-circuit voltage (V_{OC}), and maximum dark current (J_{CE}^{max}) are shown in Table 2. The maximum dark current for each cell is assumed to be the dark current at the open-circuit voltage. In addition, films deposited at 0.2, 0.6 and 3.5 sccm will be called nitrogen-doped amorphous TiO_2, nitrogen-doped anatase TiO_2 and undoped anatase TiO_2, respectively.

The results show that the higher J_{SC} was achieved for DSSC built with the nitrogen-doped anatase TiO_2. This increase in the current density is caused by the natural photoexcitation of the nitrogen states inserted in the film lattice. However, this improvement is a function of crystallinity degree and electronic defects in the film structure once J_{SC} for cell A is lower than that attained for cell B. The lower performance of cell A is attributed to the higher concentration of O vacancies in the bulk of the amorphous film. These O deficiencies generate positive holes that act as

Table 2: Short-circuit current density, open-circuit voltage, and maximum dark current for cells A, B, and C. The maximum dark current was taken for each respective V_{OC}.

DSSC	Energy band gap of the films (eV)	J_{SC} (mA/cm^2)	$\lvert V_{OC}\rvert$ (mV)	$J_{CE}{}^{max}$ (μA/cm^2)
A	1.9	1.13	747	−19.0
B	2.5	2.32	670	−31.5
C	3.2	0.62	785	−10.4

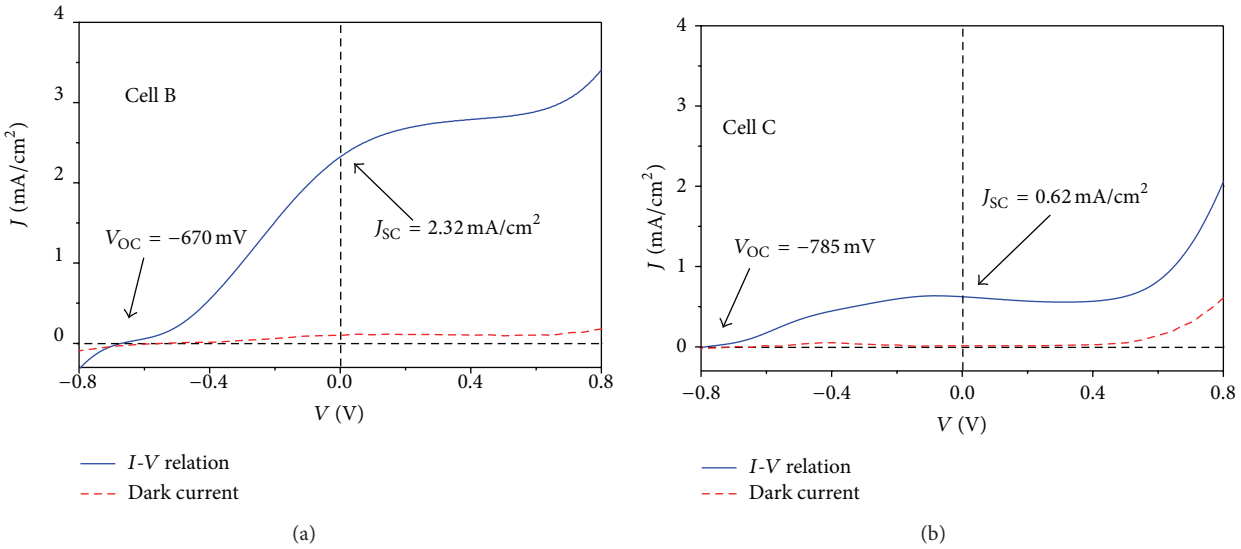

Figure 9: Current-voltage relations for cells B (with nitrogen-doped anatase TiO_2) and C (with undoped anatase TiO_2) under illuminated and dark conditions.

electron acceptor states, thus increasing the series resistance and decreasing the real cell performance. Anyway, J_{SC} for both cells A and B is higher than that obtained with cell C. This result enhances the importance of nitrogen incorporation in the film lattice.

Besides the active states Ti^{3+}, interstitial nitrogen can also act as an electron acceptor state [9, 10]. However, some studies claim that these states can also act as an electron generator state [55]. The appearance of interstitial nitrogen was confirmed by XPS and its concentration decreases as the film surface is oxidized, which indicates that films of the cells A and B have higher concentration of interstitial nitrogen than film used in cell C. As consequence, these trap states (oxygen deficiency and interstitial nitrogen) contribute to decreasing the open-circuit voltage due to lowering in the charge separation process. In addition, after nitrogen incorporation, the semiconductor-dye-electrolyte interface may have been compromised. This question was investigated by dark current measurements as follows.

Dark current is an important parameter used to evaluate the electron recombination in the semiconductor-dye-electrolyte interface between photoinjected electrons in the (nitrogen-doped) TiO_2 conduction band and triiodide ions (I_3^-). Observe that negative values for current measured under dark illumination may suggest that the film surface was not entirely covered by dye, thus exposing the semiconductor surface to the electrolyte solution and facilitating the back reaction. According to experimental setup, the color of the working electrodes was light purple, which suggests a poor adsorption of the dye molecules. The results show that the dark current was increased after nitrogen incorporation; see Table 2. This indicates that despite the fact that nitrogen increases the overall cell photocurrent, it also increases the back reaction, thereby contributing to decreasing the open-circuit voltage. Similar behavior was observed in [10]. To clarify the effect of nitrogen incorporation on the current-voltage relations of the solar cells, see Figure 9.

Some studies conducted elsewhere [56, 57] show that the conduction band edge of the TiO_2 (E_{CB}) is shifted towards negative values after nitrogen incorporation. Since the open-circuit voltage is given by $V_{OC} = E_{CB} - E_{redox}$ one can expect an increase in the V_{OC} after nitrogen incorporation since the redox potential (E_{redox}) remains unaltered. However, the opposite case was observed in this paper. This result indicates that the solid-liquid interface of the cells, produced in the present paper, was compromised not only by the nitrogen incorporation, but also by the poor adsorption of the dye molecules that increased the back reaction and reduced the open-circuit voltage.

Further studies [15, 58] claim that the surface area of TiO_2 increases after nitrogen incorporation. As consequence, this effect would increase the contact area in the solid-liquid interface and, therefore, the back reaction. In order to investigate this hypothesis, the effective surface area

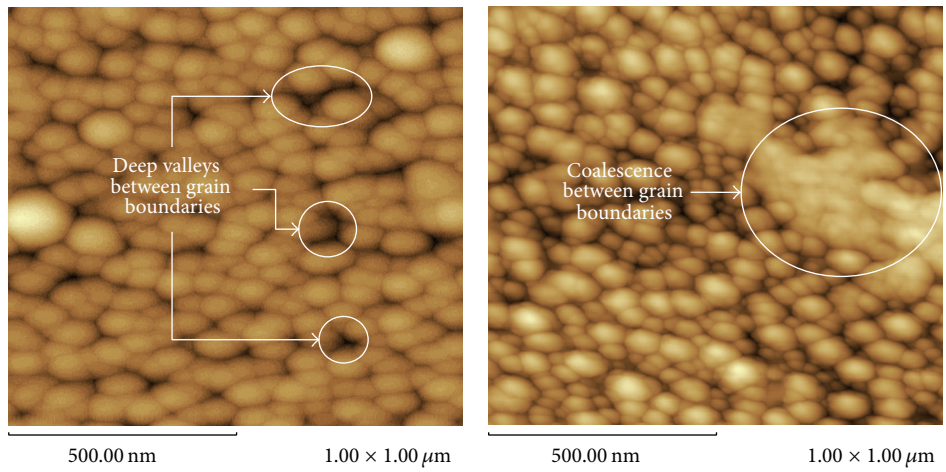

FIGURE 10: AFM images (1 μm × 1 μm) for films deposited at (a) 0.6 and (b) 3.5 sccm.

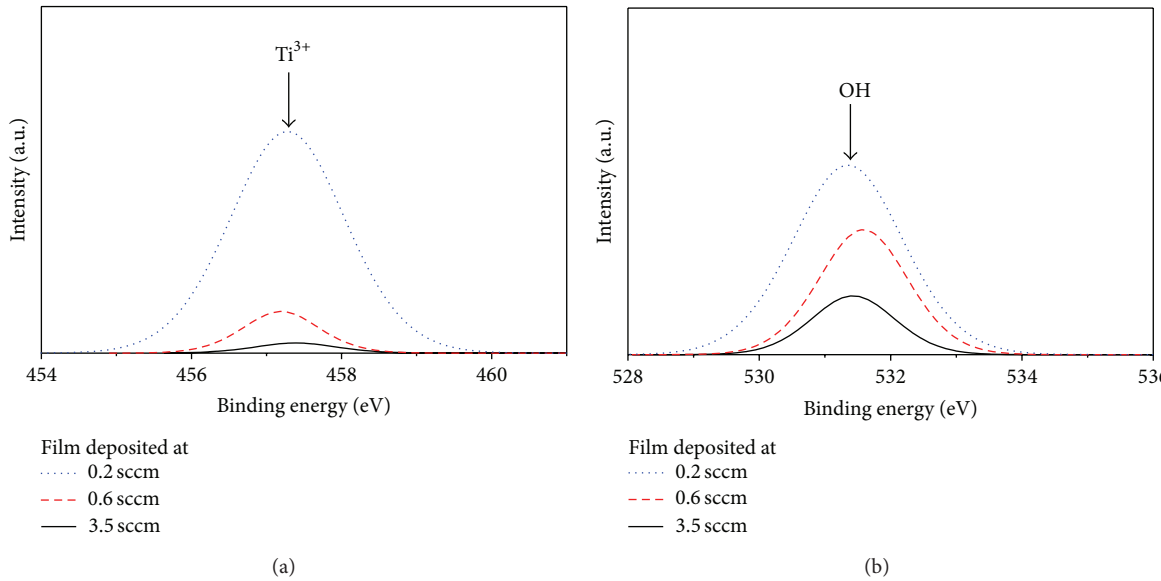

FIGURE 11: XPS spectra for (a) Ti2p$_{3/2}$ and (b) O1s core levels of the films deposited at (a) 0.2, (b) 0.6, and (c) 3.5 sccm.

of the films deposited at 0.6 and 3.5 sccm was evaluated from AFM analysis. Images (1 μm × 1 μm) are shown in Figure 10. The results show that film deposited at 0.6 sccm has an effective surface area higher (1.75 μm^2) than that deposited at 3.5 sccm (1.46 μm^2). We attribute this surface modification to the fact of nitrogen decreasing the mobility of Ti and O, thereby decreasing the diffusion process, creating deep valleys between grain boundaries and, as consequence, increasing the effective surface area. This mechanism is in agreement with that suggested in XRD analysis. At high O_2 flow rates, Ti and O diffuse easier, thus increasing the coalescence between grain boundaries and decreasing the effective surface area. See Figure 10(b).

Another important observation is described by the higher open-circuit voltage achieved for cell A in comparison to cell B. In fact, the opposite case would be expected once film used in cell A is amorphous. However, in Table 2 one can see that J_{CE}^{max} for cell A is lower than that obtained for cell B, which may explain the higher V_{OC} attained for cell A. This result suggests that the response for this question is given by physical effects happening on film surface and not into the bulk. In order to investigate this controversial result, XPS analysis was conducted. Figures 11(a) and 11(b) show the Ti2p$_{3/2}$ and O1s core levels for films deposited at 0.2, 0.6 and 3.5 sccm. As described earlier, each oxygen vacancy produces two active states Ti^{3+}. Thus, the result in Figure 11(a) indicates an increase in the number of oxygen vacancies as the films are deposited at the lowest oxygen flow rates. The appearance of these chemical states (oxygen vacancies), besides increasing the recombination processes

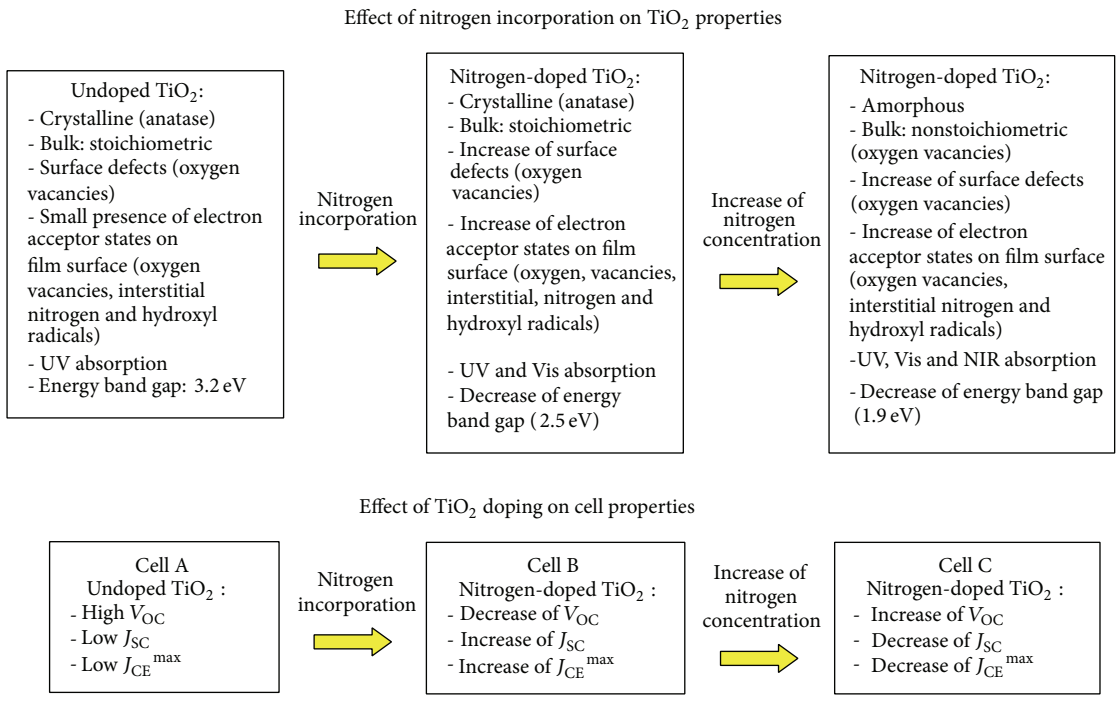

Figure 12: General properties of TiO_2 and DSSCs at different doping levels of nitrogen.

with photoelectrons, also increases the presence of hydroxyl radicals adsorbed on the film surface ; see Figure 11(b). The adsorbed OH radicals come from the dissociative adsorption of the water molecules caused by positive holes left by oxygen vacancies on its surface ($H_2O_{(ads)} + h^+_{VB} \rightarrow OH_{(ads)} + H^+_{(ads)}$). In the cases that the holes are created in the film bulk, they quickly diffuse to the film surface in a subsecond regime. During cell operation, water appearance on the TiO_2 surface might have been originated from the liquid electrolyte or solution used to dissolve the dye molecules. According to Liu and coauthors [4] the hydroxyl radicals act as a potential barrier for photoelectrons in the solid-liquid interface, thus avoiding the back reaction by blocking the reactions between these electrons and the I_3^- ions. Other studies found similar results [59, 60].

The dye molecules are mainly responsible for electric charge generation in conventional dye-sensitized solar cells , so the undoped semiconductor, in this case, is responsible only for charge transport. On the other hand, the charge generation for cells built with nitrogen-doped TiO_2 is caused by both dye molecules and the film semiconductor. For the first case, the overall electrical current produced in the solar cell is generated only by majority charge carriers. For the second one, it is generated by majority and minority charge carriers. The minority charge transport, for cells with doped films, is produced by nitrogen states in the semiconductor and the production of majority carriers remains with the dye molecules. However, if the cell built with nitrogen-doped anatase TiO_2 generates minority charge transport in the film bulk, why does this cell has achieved the higher photocurrent? To obtain this result, the electron generation rate, in the film structure, must be higher than the trapping rate. However, after absorption of solar irradiation each free electron injected in the conduction band of the film generates one positive hole in the valance band, thus creating an electron acceptor state and compensating the total charge production. Thus, this mechanism, in fact, does not explain exactly the increase of the cell photocurrent. However, in the studies conducted by Livraghi and coauthors [61], it was proposed the formation of charged diamagnetic N^- states from reoxidation of the active states Ti^{3+} ($N^\bullet + Ti^{3+} \rightarrow N^- + Ti^{4+}$). These N-induced states (N^-) are higher in energy than that of corresponding N species due to the greater Coulomb repulsion [62, 63]. According to the theory proposed by Livraghi, the formation of these doubly charged states is more favorable with the increase of Ti^{3+} [61, 63]. They also claim that the formation of these electronic states is the key factor for the improvement in the visible light activity of nitrogen-doped TiO_2 [63]. Napoli and coauthors [64] observed similar mechanism for incorporation of nitrogen species into suboxides by plasma processing. Thus, not only the incorporation of nitrogen states in the film lattice, but also the controlled presence of Ti^{3+} is a very important factor to the improvement of the DSSCs. To clarify all aspects caused by the nitrogen incorporation, a summary chart showing the evolution of the general properties of the films and cells, as the nitrogen concentration increases, is shown in Figure 12.

By this way, we conclude that nitrogen incorporated in the TiO_2 lattice by reactive sputtering acts as an efficient doping particle to improve the overall performance of dye-sensitized

solar cells, in special, the cell photocurrent. However, as the production of cells with long-term stability and in large-scale is aimed, problems in the electronic structure of TiO_2, caused by nitrogen incorporation must be roughly improved, mainly those that contribute to decreasing the open-circuit voltage. Plasma surface treatment with oxygen, for example, has achieved efficient results in decreasing the oxygen vacancies on TiO_2 surface and improving the overall cell performance [6].

4. Conclusions

In this paper, nitrogen-doped TiO_2 thin films deposited at different doping levels by DC reactive sputtering were used for fabrication of dye-sensitized solar cells. The effect of nitrogen incorporation on the general properties of the films, as well as, its effect on the working principle of the solar cells was investigated. The results indicate that the substitutional nitrogen is incorporated into TiO_2 structure from reaction with suboxides created by oxidation of the nitride layers so that the control of the reactive gas mixture, during film deposition, plays a fundamental role to achieve high doping levels. The incorporation of nitrogen particles in the film lattice shifts efficiently the absorption coefficient of the films toward the visible and near-infrared regions. However, excessive nitrogen incorporation becomes the film amorphous and leads to the appearance of excessive electron acceptor states like oxygen vacancies, interstitial nitrogen, and hydroxyl radicals. Characterization of the cells shows that nitrogen incorporated in the film structure increases the short-circuit current density due to the photoexcitation of nitrogen states in the visible part of solar spectrum. On other hand, it decreases the open-circuit voltage and increases the dark current due to the combination of several parallel effects. Among them the main ones are the increase of the electron acceptor states and the surface area of the doped films. This latter effect increases the contact area in the solid-liquid interface and, as consequence, the back reaction in the regions in which the dye molecules were not chemisorbed.

Conflict of Interests

The authors declare that there is no conflict of interest in this paper.

Acknowledgments

The authors thank FAPESP, CAPES, CNPq, and PRONEX (Grant no. 11/50773-0) for financial support; the National Institute for Space Research (INPE) for profilometry measurements; the Laboratory of Optical Surface Measurements (LMSO) of the Institute for Advanced Studies (IEAv) for spectrophotometry measurements; the University of Vale do Paraiba (UNIVAP) for XRD measurements; and the Laboratory of Nanotechnology and Solar Energy (LNES) of the University of Campinas (UNICAMP) for cells characterization. They also would like to express their special thanks to Dr. Agnaldo de Souza Gonçalves from Tezca Res. & Dev. Solar Cells Ltd. and Dr. Fábio Dondeo Origo from LMSO-IEAv for their helpful contributions.

References

[1] B. O'Regan and M. Graetzel, "A low-cost, high-efficiency solar cell based on dye-sensitized colloidal TiO_2 films," *Nature*, vol. 353, pp. 737–740, 1991.

[2] C. G. Granqvist, "Transparent conductors as solar energy materials: a panoramic review," *Solar Energy Materials and Solar Cells*, vol. 91, no. 17, pp. 1529–1598, 2007.

[3] M. Graetzel, "Dye-sensitized solar cells," *Journal of Photochemistry and Photobiology C*, vol. 4, no. 2, pp. 145–153, 2003.

[4] Y. Liu, A. Hagfeldt, X. Xiao, and S. Lindquist, "Investigation of influence of redox species on the interfacial energetics of a dye-sensitized nanoporous TiO_2 solar cell," *Solar Energy Materials and Solar Cells*, vol. 55, no. 3, pp. 267–281, 1998.

[5] S. I. Cha, Y. Kim, K. H. Hwang, Y. Shin, S. H. Seo, and D. Y. Lee, "Dye-sensitized solar cells on glass paper: TCO-free highly bendable dye-sensitized solar cells inspired by the traditional Korean door structure," *Energy and Environmental Science*, vol. 5, no. 3, pp. 6071–6075, 2012.

[6] Y. Kim, B. J. Yoo, R. Vittal, Y. Lee, N. G. Park, and K. J. Kim, "Low-temperature oxygen plasma treatment of TiO_2 film for enhanced performance of dye-sensitized solar cells," *Journal of Power Sources*, vol. 175, no. 2, pp. 914–919, 2008.

[7] A. Mathew, G. M. Rao, and N. Munichandraiah, "Effect of TiO_2 electrode thickness on photovoltaic properties of dye sensitized solar cell based on randomly oriented Titania nanotubes," *Materials Chemistry and Physics*, vol. 127, no. 1-2, pp. 95–101, 2011.

[8] Y. Yu, K. Wu, and D. Wang, "Dye-sensitized solar cells with modified TiO_2 surface chemical states: the role of Ti^{3+}," *Applied Physics Letters*, vol. 99, no. 19, Article ID 192104, 2011.

[9] R. Asahi, T. Morikawa, T. Ohwaki, K. Aoki, and Y. Taga, "Visible-light photocatalysis in nitrogen-doped titanium oxides," *Science*, vol. 293, no. 5528, pp. 269–271, 2001.

[10] S. H. Kang, H. S. Kim, J. Y. Kim, and Y. E. Sung, "Enhanced photocurrent of nitrogen-doped TiO_2 film for dye-sensitized solar cells," *Materials Chemistry and Physics*, vol. 124, no. 1, pp. 422–426, 2010.

[11] T. Ma, M. Akiyama, E. Abe, and I. Imai, "High-efficiency dye-sensitized solar cell based on a nitrogen-doped nanostructured titania electrode," *Nano Letters*, vol. 5, no. 12, pp. 2543–2547, 2005.

[12] T. Lindgren, J. M. Mwabora, E. Avendaño et al., "Photoelectrochemical and optical properties of nitrogen doped titanium dioxide films prepared by reactive DC magnetron sputtering," *Journal of Physical Chemistry B*, vol. 107, no. 24, pp. 5709–5716, 2003.

[13] S. Hashimoto, A. Tanaka, A. Murata, and T. Sakurada, "Formulation for XPS spectral change of oxides by ion bombardment as a function of sputtering time," *Surface Science*, vol. 556, no. 1, pp. 22–32, 2004.

[14] N. C. Saha and H. G. Tompkins, "Titanium nitride oxidation chemistry: an X-ray photoelectron spectroscopy study," *Journal of Applied Physics*, vol. 72, no. 7, p. 3072, 1992.

[15] G. He, L. D. Zhang, G. H. Li, M. Liu, and X. J. Wang, "Structure, composition and evolution of dispersive optical constants of sputtered TiO_2 thin films: effects of nitrogen doping," *Journal of Physics D*, vol. 41, no. 4, Article ID 045304, 2008.

[16] X. Jiang, Y. Wang, and C. Pan, "High concentration substitutional N-doped TiO_2 film: preparation, characterization, and photocatalytic property," *Journal of the American Ceramic Society*, vol. 94, no. 11, pp. 4078–4083, 2011.

[17] S. Sato, R. Nakamura, and S. Abe, "Visible-light sensitization of TiO_2 photocatalysts by wet-method N doping," *Applied Catalysis A*, vol. 284, no. 1-2, pp. 131–137, 2005.

[18] H. Irie, Y. Watanabe, and K. Hashimoto, "Nitrogen-concentration dependence on photocatalytic activity of $TiO_{2-x}N_x$ powders," *Journal of Physical Chemistry B*, vol. 107, no. 23, pp. 5483–5486, 2003.

[19] H. Li, J. Li, and Y. Huo, "Highly active TiO_2N photocatalysts prepared by treating TiO_2 precursors in NH_3/ethanol fluid under supercritical conditions," *Journal of Physical Chemistry B*, vol. 110, no. 4, pp. 1559–1565, 2006.

[20] N. Kometani, A. Fujita, and Y. Yonezawa, "Synthesis of N-doped titanium oxide by hydrothermal treatment," *Journal of Materials Science*, vol. 43, no. 7, pp. 2492–2498, 2008.

[21] S. Hu, A. Wang, X. Li, and H. Lowe, "Hydrothermal synthesis of well-dispersed ultrafine N-doped TiO_2 nanoparticles with enhanced photocatalytic activity under visible light," *Journal of Physics and Chemistry of Solids*, vol. 71, no. 3, pp. 156–162, 2010.

[22] Z. Jiang, F. Yang, N. Luo et al., "Solvothermal synthesis of N-doped TiO_2 nanotubes for visible-light-responsive photocatalysis," *Chemical Communications*, no. 47, pp. 6372–6374, 2008.

[23] L. Zhu, J. Xie, X. Cui, J. Shen, X. Yang, and Z. Zhang, "Photoelectrochemical and optical properties of N-doped TiO_2 thin films prepared by oxidation of sputtered TiN_x films," *Vacuum*, vol. 84, no. 6, pp. 797–802, 2010.

[24] L. Wan, J. F. Li, J. Y. Feng, W. Sun, and Z. Q. Mao, "Anatase TiO_2 films with 2.2 eV band gap prepared by micro-arc oxidation," *Materials Science and Engineering B*, vol. 139, no. 2-3, pp. 216–220, 2007.

[25] V. Stranak, M. Quaas, R. Bogdanowicz et al., "Effect of nitrogen doping on TiO_xN_y thin film formation at reactive high-power pulsed magnetron sputtering," *Journal of Physics D*, vol. 43, no. 28, Article ID 285203, 2010.

[26] S. H. Mohamed, O. Kappertz, J. M. Ngaruiya et al., "Influence of nitrogen content on properties of direct current sputtered TiO_xN_y films," *Physica Status Solidi A*, vol. 201, no. 1, pp. 90–102, 2004.

[27] J. M. Ngaruiya, O. Kappertz, C. Liesch, P. Müller, R. Dronskowski, and M. Wuttig, "Composition and formation mechanism of zirconium oxynitride films produced by reactive direct current magnetron sputtering," *Physica Status Solidi A*, vol. 201, no. 5, pp. 967–976, 2004.

[28] D. Herman, J. Sicha, and J. Musil, "Magnetron sputtering of TiO_xN_y films," *Vacuum*, vol. 81, no. 3, pp. 285–290, 2006.

[29] J.-M. Chappé, N. Martin, J. Lintymer, F. Sthal, G. Terwagne, and J. Takadoum, "Titanium oxynitride thin films sputter deposited by the reactive gas pulsing process," *Applied Surface Science*, vol. 253, no. 12, pp. 5312–5316, 2007.

[30] J.-M. Chappé, N. Martin, J. F. Pierson et al., "Influence of substrate temperature on titanium oxynitride thin films prepared by reactive sputtering," *Applied Surface Science*, vol. 225, no. 1–4, pp. 29–38, 2004.

[31] S. Berg and T. Nyberg, "Fundamental understanding and modeling of reactive sputtering processes," *Thin Solid Films*, vol. 476, no. 2, pp. 215–230, 2005.

[32] D. A. Duarte, J. C. Sagás, A. S. da Silva Sobrinho, and M. Massi, "Modeling the reactive sputter deposition of N-doped TiO_2 for application in dye-sensitized solar cells: effect of the O_2 flow rate on the substitutional N concentration," *Applied Surface Science*, vol. 269, pp. 55–59, 2013.

[33] Y. S. Park and H. K. Kim, "The effects of annealing temperature on the characteristics of carbon counter electrodes for dye-sensitized solar cells," *Current Applied Physics*, vol. 11, no. 4, pp. 989–994, 2011.

[34] S. R. Kim and K. M. Parvez, "Oxygen ion-beam irradiation of TiO_2 films reduces oxygen vacancies and improves performance of dye-sensitized solar cells," *Journal of Materials Research*, vol. 26, no. 8, pp. 1012–1017, 2011.

[35] M. C. Marchi, S. A. Bilmes, C. T. M. Ribeiro, E. A. Ochoa, M. Kleinke, and F. Alvarez, "A comprehensive study of the influence of the stoichiometry on the physical properties of TiO_x films prepared by ion beam deposition," *Journal of Applied Physics*, vol. 108, no. 6, Article ID 064912, 2010.

[36] Z. Zhang, X. Wang, J. Long, Q. Gu, Z. Ding, and X. Fu, "Nitrogen-doped titanium dioxide visible light photocatalyst: spectroscopic identification of photoactive centers," *Journal of Catalysis*, vol. 276, no. 2, pp. 201–214, 2010.

[37] L. Zhu, J. Xie, X. Cui, J. Shen, X. Yang, and Z. Zhang, "Photoelectrochemical and optical properties of N-doped TiO_2 thin films prepared by oxidation of sputtered TiN_x films," *Vacuum*, vol. 84, no. 6, pp. 797–802, 2010.

[38] T. L. Luke, A. Wolcott, L. P. Xu et al., "Nitrogen-doped and CdSe quantum-dot-sensitized nanocrystalline TiO_2 films for solar energy conversion applications," *Journal of Physical Chemistry C*, vol. 112, no. 4, pp. 1282–1292, 2008.

[39] Y. Nosaka, M. Matsushita, J. Nishino, and A. Y. Nosaka, "Nitrogen-doped titanium dioxide photocatalysts for visible response prepared by using organic compounds," *Science and Technology of Advanced Materials*, vol. 6, no. 2, p. 143, 2005.

[40] X. Chen and C. Burda, "Photoelectron spectroscopic investigation of nitrogen-doped titania nanoparticles," *Journal of Physical Chemistry B*, vol. 108, no. 40, pp. 15446–15449, 2004.

[41] F. Esaka, K. Furuya, H. Shimada et al., "Comparison of surface oxidation of titanium nitride and chromium nitride films studied by X-ray absorption and photoelectron spectroscopy," *Journal of Vacuum Science and Technology A*, vol. 15, no. 5, pp. 2521–2528, 1997.

[42] P. Simon, B. Pignon, B. Miao et al., "N-doped titanium monoxide nanoparticles with TiO rock-salt structure, low energy band gap, and visible light activity," *Chemistry of Materials*, vol. 22, no. 12, pp. 3704–3711, 2010.

[43] X. Chen, Y. Lou, A. C. S. Samia, C. Burda, and J. L. Gole, "Formation of oxynitride as the photocatalytic enhancing site in nitrogen-doped Titania nanocatalysts: comparison to a commercial nanopowder," *Advanced Functional Materials*, vol. 15, no. 1, pp. 41–49, 2005.

[44] N. Martin, R. Sanjinés, J. Takadoum, and F. Lévy, "Enhanced sputtering of titanium oxide, nitride and oxynitride thin films by the reactive gas pulsing technique," *Surface and Coatings Technology*, vol. 142–144, pp. 615–620, 2001.

[45] T. S. Moss, "A relationship between the refractive index and the infra-red threshold of sensitivity for photoconductors," *Proceedings of the Physical Society B*, vol. 63, no. 3, p. 167, 1950.

[46] A. Fujishima, X. Zhang, and D. A. Tryk, "TiO_2 photocatalysis and related surface phenomena," *Surface Science Reports*, vol. 63, no. 12, pp. 515–582, 2008.

[47] I. Nakamura, N. Negishi, S. Kutsuna, T. Ihara, S. Sugihara, and K. Takeuchi, "Role of oxygen vacancy in the plasma-treated

TiO_2 photocatalyst with visible light activity for NO removal," *Journal of Molecular Catalysis A*, vol. 161, no. 1-2, pp. 205–212, 2000.

[48] T. Lindgren, J. Lu, A. Hoel, C. G. Granqvist, G. R. Torres, and S. E. Lindquist, "Photoelectrochemical study of sputtered nitrogen-doped titanium dioxide thin films in aqueous electrolyte," *Solar Energy Materials and Solar Cells*, vol. 84, no. 1–4, pp. 145–157, 2004.

[49] D. A. Duarte, M. Massi, and A. S. da Silva Sobrinho, "Comparison between conventional and hollow cathode magnetron sputtering systems on the growing of titanium dioxide thin films: a correlation between the gas discharge and film formation," *European Physical Journal—Applied Physics*, vol. 54, no. 2, Article ID 20801, 2011.

[50] D. R. Irala, H. S. Maciel, D. A. Duarte, M. Massi, and A. S. da Silva Sobrinho, "Influence of the nitrogen concentration on the photoinduced hydrophilicity of N-doped titanium dioxide thin films deposited by plasma sputtering," *ECS Transactions*, vol. 31, no. 1, pp. 109–115, 2010.

[51] K. Prabakar, T. Takahashi, T. Nezuka et al., "Visible light-active nitrogen-doped TiO_2 thin films prepared by DC magnetron sputtering used as a photocatalyst," *Renewable Energy*, vol. 33, no. 2, pp. 277–281, 2008.

[52] J. Muscat, V. Swamy, and N. M. Harrison, "First-principles investigations for $YH_3(YD_3)$: energetics, electric-field gradients, and optical properties," *Physical Review B*, vol. 65, no. 22, Article ID 224112, 9 pages, 2002.

[53] B. A. Nejand, S. Sanjabi, and V. Ahmadi, "Optical and photocatalytic characteristics of nitrogen doped TiO_2 thin film deposited by magnetron sputtering," *Scientia Iranica*, vol. 17, no. 2, pp. 102–107, 2010.

[54] K. Hukari, R. Dannenberg, and E. A. Stach, "Nitrogen effects on crystallization kinetics of amorphous TiO_xN_y thin films," *Journal of Materials Research*, vol. 17, no. 3, pp. 550–555, 2002.

[55] C. Di Valentin, G. Pacchioni, A. Selloni, S. Livraghi, and E. Giamello, "Characterization of paramagnetic species in N-doped TiO_2 powders by EPR spectroscopy and DFT calculations," *Journal of Physical Chemistry B*, vol. 109, no. 23, pp. 11414–11419, 2005.

[56] K. Yang, Y. Dai, and B. Huang, "Study of the Nitrogen Concentration Influence on N-Doped TiO_2 Anatase from First-Principles Calculations," *Journal of Physical Chemistry C*, vol. 111, no. 32, Article ID 12086, 2007.

[57] P. Xiang, X. Li, H. Wang et al., "Mesoporous nitrogen-doped TiO_2 sphere applied for quasi-solid-state dye-sensitized solar cell," *Nanoscale Research Letters*, vol. 6, article 606, 2011.

[58] S. W. Park and J. E. Heo, "Characteristics of N-doped titanium oxide prepared by the large scaled DC reactive magnetron sputtering technique," *Separation and Purification Technology*, vol. 58, no. 1, pp. 200–205, 2007.

[59] P. V. V. Jayaweera, P. K. D. D. P. Pitigala, M. K. I. Seneviratne, A. G. U. Perera, and K. Tennakone, "1/f noise in dye-sensitized solar cells and NIR photon detectors," *Infrared Physics and Technology*, vol. 50, no. 2-3, pp. 270–273, 2007.

[60] Y.-S. Jung, B. Yoo, M. K. Lim, S. Y. Lee, and K.-J. Kim, "Effect of Triton X-100 in water-added electrolytes on the performance of dye-sensitized solar cells," *Electrochimica Acta*, vol. 54, no. 26, pp. 6286–6291, 2009.

[61] S. Livraghi, M. C. Paganini, E. Giamello, A. Selloni, C. Di Valentin, and G. Pacchioni, "Origin of photoactivity of nitrogen-doped titanium dioxide under visible light," *Journal of the American Chemical Society*, vol. 128, no. 49, pp. 15666–15671, 2006.

[62] S. Hoang, S. P. Berglund, N. T. Hahn, A. J. Bard, and C. B. Mullins, "Enhancing visible light photo-oxidation of water with TiO_2 nanowire arrays via cotreatment with H_2 and NH_3: synergistic effects between Ti^{3+} and N," *Journal of the American Chemical Society*, vol. 134, no. 8, pp. 3659–3662, 2012.

[63] C. Di Valentin, E. Finazzi, G. Pacchioni et al., "Density functional theory and electron paramagnetic resonance study on the effect of N-F codoping of TiO_2," *Chemistry of Materials*, vol. 20, no. 11, pp. 3706–3714, 2008.

[64] F. Napoli, M. Chiesa, S. Livraghi et al., "The nitrogen photoactive centre in N-doped titanium dioxide formed via interaction of N atoms with the solid. Nature and energy level of the species," *Chemical Physics Letters*, vol. 477, no. 1–3, pp. 135–138, 2009.